COMPUTER METHODS AND PROGRAMS IN BIOMEDICINE XXX (2011) XXX–XXX

journal homepage: www.intl.elsevierhealth.com/journals/cmpb

Simple methods for segmentation and measurement of diabetic retinopathy lesions in retinal fundus images

Cemal Köse[a,*], *Uğur Şevik*[b], *Cevat İkibaş*[a], *Hidayet Erdöl*[c]

[a] *Department of Computer Engineering, Faculty of Engineering, Karadeniz Technical University, 61080 Trabzon, Turkey*
[b] *Department of Statistics and Computer Sciences, Faculty of Arts and Sciences, Karadeniz Technical University, 61080 Trabzon, Turkey*
[c] *Department of Ophthalmology, Faculty of Medicine, Karadeniz Technical University, 61080 Trabzon, Turkey*

ARTICLE INFO

Article history:
Received 7 June 2010
Received in revised form
16 June 2011
Accepted 17 June 2011

Keywords:
Automatic diagnosis of DR
Automatic segmentation
Background image extraction
DR
Medical image analysis
Optic disc
Retinal images

ABSTRACT

Diabetic retinopathy (DR) is one of the most important complications of diabetes mellitus, which causes serious damages in the retina, consequently visual loss and sometimes blindness if necessary medical treatment is not applied on time. One of the difficulties in this illness is that the patient with diabetes mellitus requires a continuous screening for early detection. So far, numerous methods have been proposed by researchers to automate the detection process of DR in retinal fundus images. In this paper, we developed an alternative simple approach to detect DR. This method was built on the inverse segmentation method, which we suggested before to detect Age Related Macular Degeneration (ARMDs). Background image approach along with inverse segmentation is employed to measure and follow up the degenerations in retinal fundus images. Direct segmentation techniques generate unsatisfactory results in some cases. This is because of the fact that the texture of unhealthy areas such as DR is not homogenous. The inverse method is proposed to exploit the homogeneity of healthy areas rather than dealing with varying structure of unhealthy areas for segmenting bright lesions (hard exudates and cotton wool spots). On the other hand, the background image, dividing the retinal image into high and low intensity areas, is exploited in segmentation of hard exudates and cotton wool spots, and microaneurysms (MAs) and hemorrhages (HEMs), separately. Therefore, a complete segmentation system is developed for segmenting DR, including hard exudates, cotton wool spots, MAs, and HEMs. This application is able to measure total changes across the whole retinal image. Hence, retinal images that belong to the same patients are examined in order to monitor the trend of the illness. To make a comparison with other methods, a Naïve Bayes method is applied for segmentation of DR. The performance of the system, tested on different data sets including various qualities of retinal fundus images, is over 95% in detection of the optic disc (OD), and 90% in segmentation of the DR.

1. Introduction

Digitized data in ophthalmology attracts more and more researchers for automatic segmentation and measurement of some important diseases such as DR and ARMD lesions. DR and other eye diseases are characterized by structural variations in retina, which are exploited in automated diagnosis systems. Since the DR is developed in diabetics in a long period of time, continuous monitoring of eyes is extremely

* *Corresponding author*. Tel.: +90 4623773167; fax: +90 4623257405.
E-mail addresses: ckose@ktu.edu.tr (C. Köse), usevik@ktu.edu.tr (U. Şevik), cikibas@ktu.edu.tr (C. İkibaş), herdol@ktu.edu.tr (H. Erdöl).
0169-2607/$ – see front matter © 2011 Elsevier Ireland Ltd. All rights reserved.
doi:10.1016/j.cmpb.2011.06.007

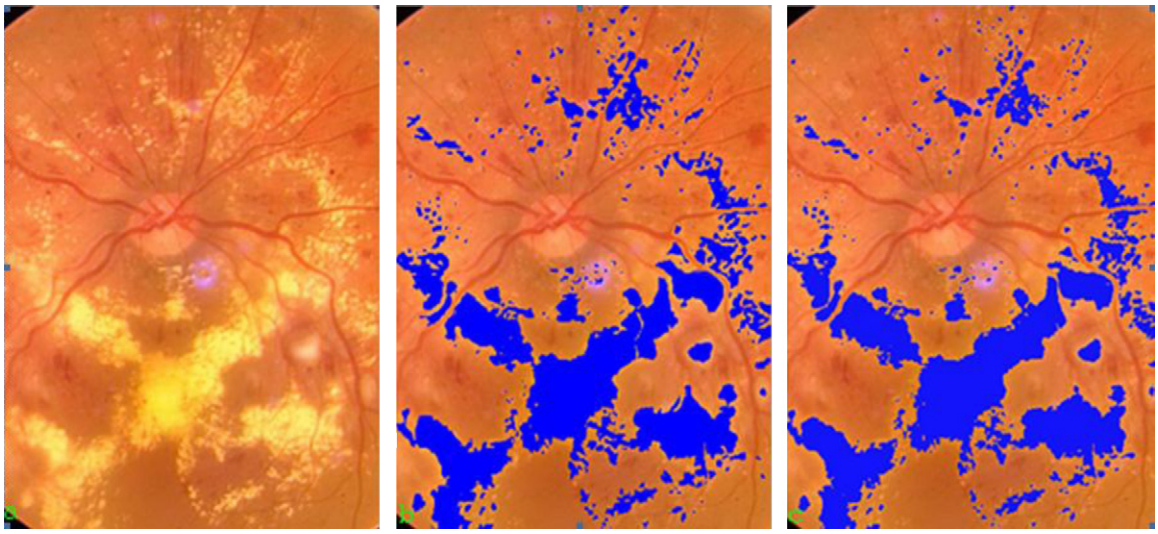

Fig. 1 – (a) An original image, and (b) manual and (c) automatic segmentation results of the image.

important to diagnose the early symptoms and take necessary precautions for an effective treatment [1–3]. The early treatment may avoid or reduce blindness. On the other hand, standard grading system is used in assessing images manually, which requires ophthalmologist or professionally trained graders to analyze large number of retinal fundus images [4,5]. An original image (a), its manual (b) and automatic segmentation results (c) are given in Fig. 1. Manual segmentation and measurement of the diseases as in the figure are quite difficult, and user may easily make mistakes during the operation [2,3,6]. Quality of segmentation also changes depending on quality of image, and ability and experience of user. The manual process can take up to an hour for two eyes. Therefore, a fully automated system segmenting the diseases in retinal images could definitely reduce the workload of clinicians. The image may be segmented and measured by the system first and then checked by a medical professional if further analysis is necessary upon the automatic classification of image as abnormal. It should also be perceived that these kinds of automated systems cannot fully be trusted in detection of illness or locating a specific region such as OD or macula. That is why a medical professional performs a last check on detected abnormality on images. To give an example, considering all the optic disc detection methods developed so far, none of those methods can 100% guarantee detecting the optic disc or finding the exact location of OD in any conditions without any restriction such as image conditions and quality, structure of degenerations, and the way the image is taken. Apart from automated system, highly experienced physicians can even make mistakes in detecting the OD in problematic or low quality retinal images.

Recent investigations have shown that the pathological diseases such as DR can be measured from retinal fundus images [5,7–12]. Quantifying the problems in images will enable the evaluation of the course of retinal diseases. Consequently, there is a strong demand for automated diagnosis and measurement processes [4,10,13–16]. However, segmenting, measuring and monitoring the development of degenerations such as hard exudates, cotton wool spots, MAs, and HEMs related with DR, are quite difficult because of irregular pattern of degenerations [17–19]. In other words, one common problem, encountered during segmentation of lesions, is the non-uniformity of the DR. Currently a number of semi-automated methods are used for segmentation and detection of DR [8,20–22]. Five previous methods are examined in retinopathy in [13]. In the first method, using a three class Gaussian mixture model, a group of MA candidates are segmented by thresholding fitted model. Logistic regression is used to generate likelihood for the places that may be MA. Second method presented in the paper employs feature extraction to determine the candidate places and Bayesian classifier to assign likelihood to each one to be MAs. The third method uses template matching in the wavelet domain and the fourth method uses multi scale Bayesian correlation filtering approach to find MA candidates. MA detection method based on double ring filter is used in the last method presented in [13]. Another study employs neural network classifier in order to detect hard exudates in retinal images. This study employs an algorithm which includes a neural network classifier for this task. Three classifiers were investigated: multilayer perceptron, radial basis function and support vector machine (SVM) are used in this study [23]. To detect the hard exudates, a group of features was extracted from image regions, and the subset which was best discriminated between exudates and retinal background was selected by means of logistic regression after applying normalization on the image and segmenting the candidate regions. Lastly, noisy regions are eliminated by applying post-processing on the image [17]. Another study first employs image enhancement, shade correction and image normalization as preprocessing methods on the image. The study then applies diameter closing and an automatic threshold scheme for detection of candidate regions for MA. Then, the candidate regions are classified as MA and non-MA by using feature extraction method [14]. A template matching technique using optimal wavelet transformation for detecting MAs in retinal images is employed in [24].

Please cite this article in press as: C. Köse, et al., Simple methods for segmentation and measurement of diabetic retinopathy lesions in retinal fundus images, Comput. Methods Programs Biomed. (2011), doi:10.1016/j.cmpb.2011.06.007

A multi-scale amplitude-modulation–frequency-modulation method was also proposed for discriminating between normal and pathological retinal images [25]. Most of these methods detect only one type of lesions of DR such as MAs and hard exudates, and they require user intervention.

Retinal degenerations are quite irregular and complex structures. Thus, successful segmentation of these irregular structures requires very complex and costly methods. On the other hand, healthy textures of retinal images have very regular patterns, and segmenting these regular patterns is easier than that of the irregular patterns. In the literature, many methods have been proposed for segmenting retinopathy but these methods are not efficient in full segmentation of pathological structures because of the irregularities and complexities of the structures of the degenerations. In this study, an inverse method for segmentation and measurement of bright lesions, and a simple method utilizing the background image for measuring dark lesions are proposed to detect DR lesions in retinal fundus images. These methods are relatively more effective and less costly, thus more promising compared to the previous methods because of their simplicity.

The rest of this paper is organized as follows. A summary of the other segmentation approaches proposed in other studies for DR lesions is given in Section 2. An overview of the implementation details of the developed system and basic techniques used in the segmentation such as determining background image, locating optic disk and eliminating vessels are given in Section 3. The region growing method, the region growing method with background correction, the adaptive region growing method with background correction for segmentation of bright lesions of DR, and the threshold based method for segmentation of the dark lesions of DR are also explained in the same section. Measurement and evaluation methods are presented in the same section. Measurements of DR and evaluation of course of the disease are explained in Section 4. The results are discussed in Section 5. The conclusions and future work are given in Section 6.

2. Previous approaches for screening the DR in retinal fundus images

Many methods have been proposed for detecting, segmenting DR related lesions, screening DR, detecting OD and eliminating vessels in retinal images since the researches were started on automated monitoring systems in ophthalmology [10,16,26–28]. Most of these methods are based on the techniques such as segmentation, edge detection, mathematical and tracking models, 2D matched filters and image thresholding methods [11,19,29–31]. Automatic model based detecting, pattern recognition, texture analysis, mathematical morphology methods and diagnosis approaches were also proposed for screening DR lesions. Some of these techniques work on anatomic location detection in retinal images [27,32]. Besides they usually focus on detection and segmentation of only one anatomical structure such as OD or blood vessels [32–39]. Additionally, some methods detecting one or more features and abnormalities in retinal images are introduced in [1,30,40,41]. A multi-layer perceptron neural net using the inputs derived from a principal component analysis for edge detection in retinal image was employed for OD detection in [42]. Model based approaches are proposed for detecting OD, fovea and some other features in retinal images [27,32]. Additionally, computer based methods for detecting MAs were developed in [14,24,43,44]. Many other approaches have been proposed for automatic identification of some features of DR [10,15,19,45].

Even though many methods have been proposed in the field, those methods are limited by at least one of the following drawbacks. Firstly, user involvement is needed to select region of interest and the methods are not completely automatic. Secondly, under varying image conditions, lack of adaptive capabilities may result in poor quality of segmentation such as local, over and under segmentations. Thirdly, most of the previous segmentation methods are only applicable to not all types of lesions but one or two types of DR lesions. Lastly, segmentation processes in proposed applications require large computational efforts.

3. Techniques used in segmentation of DR

Several preprocessing and utility techniques are employed for automatic segmentation of DR. These are called background image extraction method, OD detection method and vessel elimination methods. In the application, images are first converted to 8-bit gray scale images. Then background image of healthy parts of image is extracted from the gray scale retinal image, and then the healthy parts are extended to the whole image. The extended background image is used in the segmentation. Thus, the region growing approach exploits the background image for a dynamic segmentation. A method for OD detection is developed for locating OD and eliminating OD area from the segmented image. In addition to these, a vessel elimination technique is also employed to eliminate vessel structures from the final segmented image. Taking advantages of these preprocessing techniques, three inverse segmentation methods are proposed for segmenting DR. These are region growing method, region growing method with background correction, and adaptive region growing method with background correction. Naïve Bayes method is applied to evaluate the performance of the methods in segmentation of DR.

In this study, several methods have been proposed for automatic segmentation of DR lesions. Most important of these are background image calculation method, inverse segmentation methods with adaptive region growing and background correction, and background threshold based method for segmenting lesions such as MAs and HEMs. Our system first generates the reference or extended background image from a retinal image. Healthy parts of the retinal image except for vessel and OD areas are used in the calculation of this reference image. Then, the retinal image is divided into two parts as low and high intensity areas based on the intensities of the background image. So, the background image is used as the dynamic threshold value while segmenting high intensity (bright) degenerations in the image. Then the bright degenerations are segmented separately by using the inverse segmentation method and dynamic thresholding. The method takes advantage of using the dynamic threshold to adapt itself to intensity changes across the whole image and

Please cite this article in press as: C. Köse, et al., Simple methods for segmentation and measurement of diabetic retinopathy lesions in retinal fundus images, Comput. Methods Programs Biomed. (2011), doi:10.1016/j.cmpb.2011.06.007

generates promising segmentation results. Unlike the previous studies based on segmentation of unhealthy regions, the inverse method first segments healthy parts and then inversely segments unhealthy parts of the retinal images. The direct segmentation methods segmenting DR are more complex and costly than our method because the texture of unhealthy areas of retina is quite irregular. Morphologic properties of degenerated areas such as chromatic colors, gradient of color, and border structure vary dramatically. These kinds of structures increase the complexity of the feature extraction, training and segmentation processes for measuring DR. Therefore, the inverse segmentation method, taking advantage of homogeneity of the structure of healthy areas, is employed since it is simple and it generates more accurate results.

For segmenting degenerations with low intensities (dark), a simple method is employed. Low intensity regions usually consist of vessels and dark lesions. Therefore, a vessel segmentation method [46] is first applied and vessels are eliminated from the retinal image. After eliminating the vessels, low intensity regions would include only the dark lesions that can be classified as MAs and HEMs. Therefore, all degenerations in a retinal image can be segmented, measured and monitored at the same time. In other words, our system measures the total changes in the degenerations across the whole retinal image quite successfully. The proposed approach is also able to locate OD and eliminate OD area in retinal image. Complete analysis of retinal image can be done in several seconds without any user involvement by using the developed application.

Basic steps in our automatic screening system for DR are as the following;

- Extracting background image of healthy areas and extending it across the whole image.
- Determining low and high intensity regions of the image.
- Segmenting bright lesions by applying the inverse adaptive region growing method.
- Segmenting the dark lesions.
- Eliminating the vessels.
- Detecting the OD and eliminating the OD area.
- Calculating percentages of healthy and unhealthy parts of the image.
- Comparing segmentation results with images taken in previous occasions.
- Generating quantitative results to diagnose or evaluate the progress of the illness.

Low and high intensity regions on the image can be differentiated from background image determined from healthy regions except vessels and OD area. A block diagram of the processes is given in Fig. 2.

3.1. *Preprocessing and utility techniques for segmenting DR*

Several utility techniques are employed in segmentation of DR. These are extraction of the background image and then extending it to the whole image, OD localization and OD area elimination, and vessel elimination techniques. Then, segmentation methods are applied separately for segmentation of dark and bright lesions.

3.1.1. *Calculation of background image*

An inverse segmentation method is proposed for segmenting ARMD by Köse et al. [4,9]. The method is quite simple and successful in segmenting degenerations in the macular area. Thus, the intensity changes in the macular area can easily be tolerated by region growing method because the intensity changes in the macular area are smaller than that of changes in the whole retinal image. In the application, region growing method iteratively examines neighboring pixels around the initial set of seed pixels according to similarity constraints. Thus, it expands the region by adding similar adjacent pixels. This process continues until all pixels are classified to be combined with healthy or unhealthy region. On the other hand, unlike ARMD segmentation, not only the macular area but also the complete retinal image is considered in segmentation of DR lesions. In some cases, intensity changes in a complete retinal image may not be easily tolerated by a simple region growing method. In the application, lesions in the macular area are quite successfully segmented but some lesions in other parts of the image are not segmented as good as macular area. The inverse method in [4,9] itself as a standalone approach, developed to detect ARMD, was not that successful in detection of DR. So we needed to make some improvement in the method to get a better result for DR. In this study, one of the improvements is calculating and using the background image in detection of DR, which presents adaptive techniques to segment DR lesions more accurately.

In the application, it was seen that the region growing method cannot segment the lesions with dramatic background intensity changes. The performance of the method also depends on the seed pixels chosen as the starting points of region growing. In this application, intensity of the healthy areas in the images determines the background image. If the region growing method dynamically adapts itself according to the background image, it may segment the whole image successfully. Hence, we state that the background image of unhealthy areas can be extracted based on the healthy part of the retinal image as given in Fig. 3. In order to do this, healthy parts of the retinal image are first extracted and then the average intensity of healthy parts is calculated. Finally, these healthy parts are extended to the whole image by considering the distances between healthy parts and current pixel as shown in Fig. 3. Therefore the background image of unhealthy parts is also constructed to be employed in segmentation of DR, which is an improvement to the existing method presented in [4,9].

Retinal images consist of healthy textures, unhealthy textures, blood vessels and some other degeneration. A typical square sample of healthy texture can be considered as the Characteristic Image (CI) of the texture. Some statistical properties of CIs are the average of variation intervals of intensities, the average of standard intensity deviation intervals, intensity distribution, and high and low extreme intensity distributions of the texture. These properties are collected from a typical region or interested regions of images in training data set chosen by user during the training period. In the application, CIs of healthy texture are determined. Then, the healthy texture

Please cite this article in press as: C. Köse, et al., Simple methods for segmentation and measurement of diabetic retinopathy lesions in retinal fundus images, Comput. Methods Programs Biomed. (2011), doi:10.1016/j.cmpb.2011.06.007

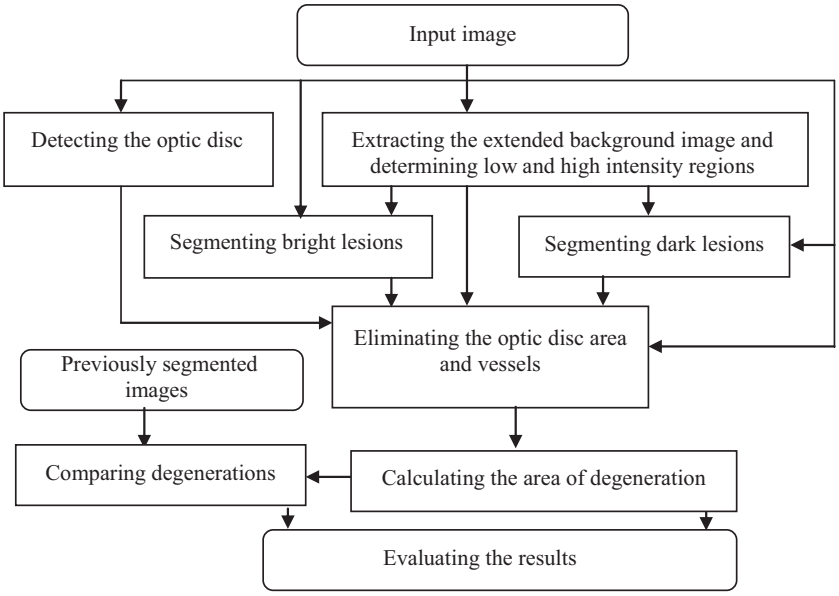

Fig. 2 – A block diagram of the process followed in developed application.

for the current image may be automatically determined by using intensity distributions and parameters of healthy textures obtained from the training data set. In this work, twelve healthy sample images consisting of various qualities of retinal images are chosen as the training set. This statistical technique was also employed in segmentation of bone textures in MR images [47], and retina texture in retinal fundus images [4,9], previously. Our experiments show that intensity distribution of the CIs of the healthy retinal texture is a Gaussian distribution with a standard deviation of 3.5 and an average intensity value of 127, shown in Fig. 3(a). As seen in the figure, not the whole distribution (0–255) but the center of the distribution is focused. For example, a typical intensity distribution from 120 to 130 is shown in the figure. These values are used in determination of the healthy background images in this application. In other applications, the intensity distributions of the CIs (monochrome image) are first calculated from the healthy textures chosen for training by user. In this application, only one CI is used for all images without user involvement. Then, intensity distributions of all images, sized in the range of 2×2–50×50 pixels, are calculated by using Eq. (1). But, only the intensity distributions of CIs which are the Gaussian distribution are used during the segmentation. In this application, CI with standard deviation of 3.5 is the same for all images and the size of the CI is also set to 10×10 pixels for all images. The size of the CI is important because if the size is chosen very large, most of the background image will be lost and little background image is extracted. On the other hand, if the size of the CI is chosen very small, some unhealthy parts of the image may be classified as healthy and the background image may include unhealthy parts. Therefore, the size of background image is set experimentally and the intensity distribution of the CI for that size is registered as integer arrays. These arrays are normalized for the comparison in the

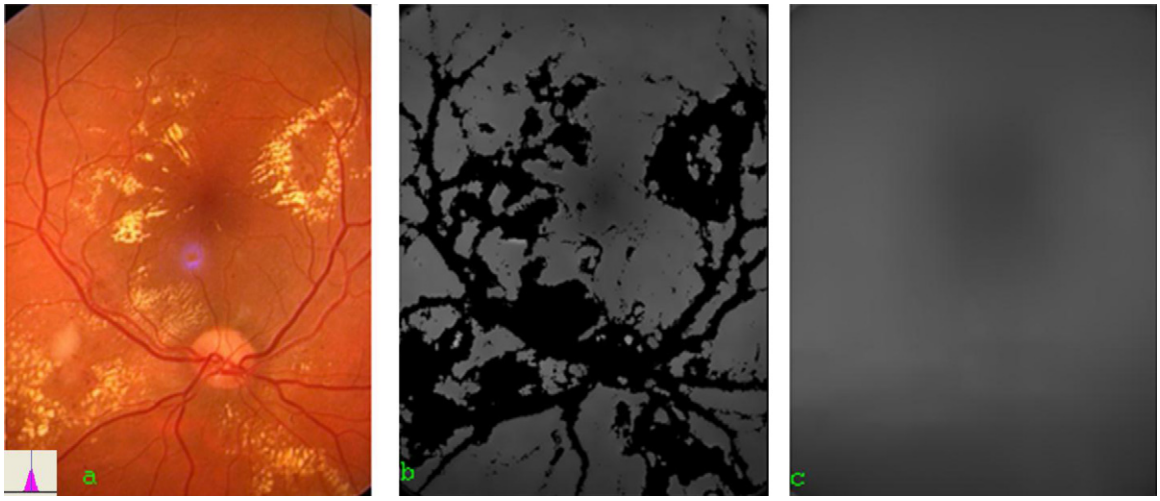

Fig. 3 – (a) An original image and (b) basic background image (c) extended background image.

Please cite this article in press as: C. Köse, et al., Simple methods for segmentation and measurement of diabetic retinopathy lesions in retinal fundus images, Comput. Methods Programs Biomed. (2011), doi:10.1016/j.cmpb.2011.06.007

extraction. The intensity distributions are calculated by using Eq. (1).

$$Int\_Dist[k]_l = \sum_{i=0}^{M}\sum_{j=0}^{N}\{Int\_Dist[Int(i,j)]_l + 1\} \quad (1)$$

where M and N are the height and width of the CI, respectively. $Int\_Dist[\,]$ is the intensity distribution, (i,j) is coordinate of the current pixel, subscription l represents the size of CI, and k stands for intensity value index which is $Int(i,j)$.

The proposed method is employed to extract the background image of healthy area of the whole retinal image. Intensity distribution of current sample area on current pixel is calculated, normalized and compared with the CI distribution. The size of sample area is set to the value of the size of CI. In other words, the sample area, representing the current area, will be compared with the CI in calculation of the healthy background image. An extracted background image is given in Fig. 3(b). In the application, one intensity index is set as reference point. The reference point is the mean index of the distributions. Two distributions are overlapped so that the reference point met with the corresponding one. Thus, the intensity distribution of current area is shifted for the comparison with the CI intensity distribution. Then, the differences between intensity distributions are calculated by using Eq. (2). If the difference between the distributions is less than a threshold value, intensity of current pixel is set to the average intensity value of the sample area on the background image. Otherwise, it is set as empty pixels (pixels with no intensity value) and set to the lowest intensity value.

$$\{Dist\_Diff\_Err\}_l = \sum_{i=a}^{b}|\{[Int\_Dist(i)_{CI}]_l - [Int\_Dist(i)_{Sample}]_l\}| \quad (2)$$

where $\{Dist\_Diff\_Err\}_l$ called Distribution Difference Error, is the difference between the intensity distributions of CI and current sample image in size l, $Int\_Dist()_{CI}$ is the intensity distributions of CI, and $Int\_Dist()_{Sample}$ is the intensity distribution of current sample image. In Eq. (2), i is the intensity index, varying between a and b, where a is the smallest ($a \geq 0$) and b is the greatest common intensity index of both distributions ($b \leq 255$).

As illustrated in Fig. 4, the extracted background image generated based on healthy region is not complete and has many areas without a background value because of unhealthy regions. The proposed techniques, adapting itself according to the background image, may fail in these areas with no background value if the background image cannot be fully completed. Therefore, the background image should be extended to these areas by using Eq. (3). In the application, four neighboring pixels of the current empty pixel are interpolated to calculate background intensity value of the current pixel. If one of the neighboring pixels has no background value, that neighborhood is extended to the neighboring pixel by doubling the size of the neighbor in that direction, which is illustrated in Fig. 4. The average intensity of the background pixels in the doubled area (except for the empty pixels) is only considered as the intensity of the neighboring area and the distance from the current pixel to the middle of the doubled neighboring area is accounted in the calculation of the intensity value of the current pixel. This process is carried out for all empty pixels until reaching a certain size or finding at least one non-empty pixel. If this process is not successful for some neighboring pixels, the average value of the other neighboring pixels is accounted in the calculation. This means that none of the pixels in the neighboring area is healthy. The distances of the doubled neighboring pixels are used in the calculation. Then, the extended image is calculated by using Eq. (3). Finally, a simple averaging filter using weighted average of current and surrounding pixels are used to filter the extended image.

$$Im\ g(i,j) = \left\{ \frac{\sum_{k=1}^{ng}[Int\_neighbor(k)/d(k)]}{\sum_{k=1}^{ng}[1/d(k)]} \right\} \quad (3)$$

where (i,j) stands for the current pixel and $Im\,g(i,j)$ represents the extended image. $Int\_neighbor(k)$ represents the intensity value of the neighboring pixels and $d(k)$ is the distance from the current pixel to the middle of the neighboring pixels. ng, representing the number of the neighboring areas, is set to 4 in this application, experimentally. In other words, the number of neighboring area is the number of neighborhood used in the extension process. Here, many experiments were performed to determine the number of neighboring area to be chosen that gives the best results. As a result of the tests we concluded that choosing 4 generates better results.

3.1.2. Method for locating the OD

OD in a retinal fundus images is one of the most known invariants. Therefore the detection of the OD is important in analyzing and quantifying objects and lesions in the retinal images. This enables the user to analyze images automatically in a short time, and avoid inter/intra-observer variability. ODs in the retinal images have many distinctive properties that can be utilized in their detection. These distinct properties are their circular geometric structure, high intensity, blood vessel structure and such. In the literature, many techniques are used to detect [27,28,32,36] and segment [16,48,49] the OD in retinal fundus images. In this application, an edge detection filter, expressed in Eq. (4), which is called "Modified Sobel Operator" that makes edges on the image more evident, is employed to detect edges in the fundus images as illustrated in Fig. 5.

$$Im\,g\_filtered(i,j) = \frac{\sum_{k=1}^{n} abs[Im\,g\_v\_filter(i+k,j)] + abs[Im\ g\_h\_filter(i,j+k)]}{n} \quad (4)$$

where k stands for the distance shown in Fig. 5, (i,j) stands for current pixel and $Im\,g\_filtered(i,j)$ represents the filtered image. $Im\ g\_v\_filter(i+k,j)$ and $Im\,g\_h\_filter(i,j+k)$ represent the vertical and horizontal Sobel operations, respectively.

In Eq. (4), n is experimentally set to 3 to make the vessel edges more apparent on the resulting image so that the intensity changes and edges around the OD could be used to determine the location of the OD. In this process, especially vessels on OD region provide distinctive features about the position of the OD. In order to utilize those properties, the histogram of filtered image is calculated as in Fig. 6. The max-

Please cite this article in press as: C. Köse, et al., Simple methods for segmentation and measurement of diabetic retinopathy lesions in retinal fundus images, Comput. Methods Programs Biomed. (2011), doi:10.1016/j.cmpb.2011.06.007

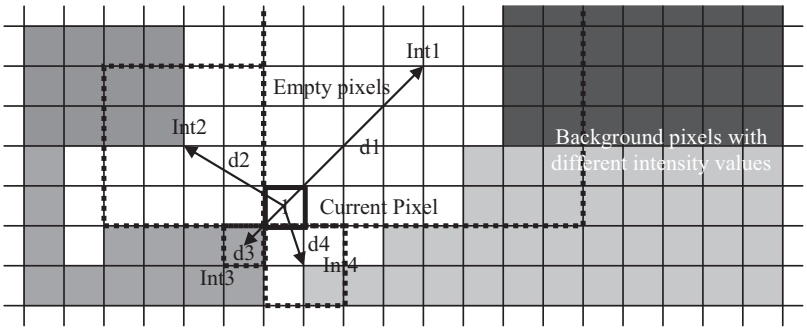

Fig. 4 – Extending the background image.

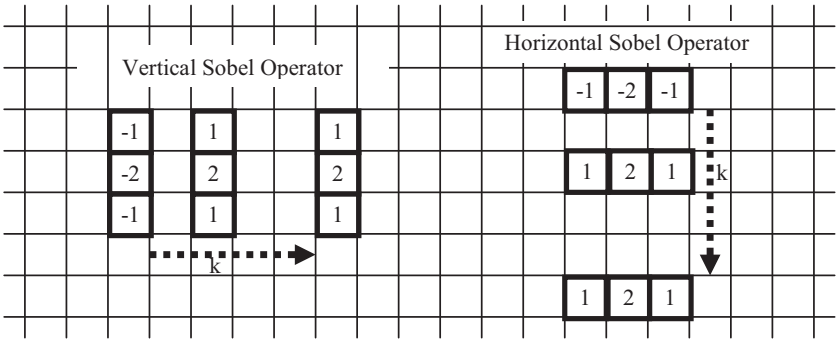

Fig. 5 – The Modified vertical and horizontal Sobel Operators.

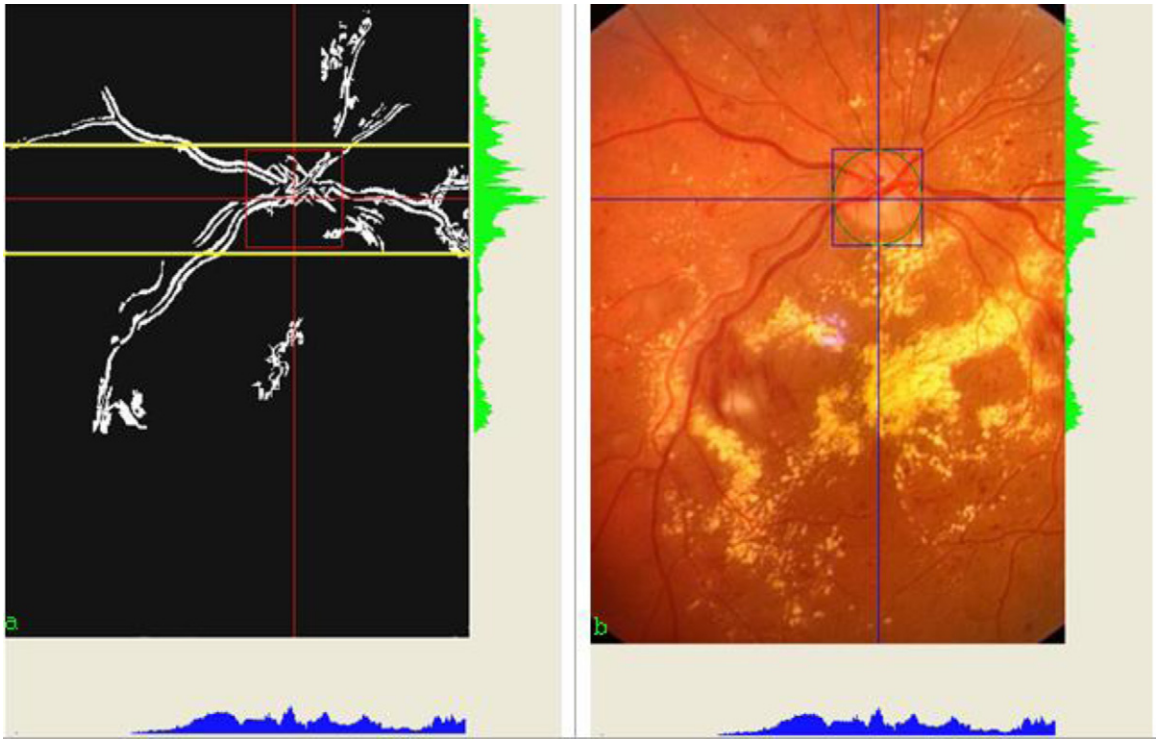

Fig. 6 – (a) Detection of the OD and (b) determination of the OD area.

Please cite this article in press as: C. Köse, et al., Simple methods for segmentation and measurement of diabetic retinopathy lesions in retinal fundus images, Comput. Methods Programs Biomed. (2011), doi:10.1016/j.cmpb.2011.06.007

imum values of the horizontal histogram of the filtered image and vertical histogram of the strip around OD are determined to locate the OD. Here, the vertical position of the OD (vertical center of OD as shown in the figure) is first calculated from the vertical histogram, and then the horizontal strip around the OD is placed. The yellow lines show the upper and lower borders of the strip, and red lines show the maximum values of the histograms and location of OD. The size of the strip is chosen a little bit larger than the diameter of a typical OD, which is set to 90 pixels in our case, to include edges of the OD as well.

A block diagram for finding OD location is given in Fig. 7. The input image is firstly filtered by using the modified Sobel filter, and unexpected high intensity areas in the original image are determined related to the background image [50]. These high intensity areas, apart from the vessels, are removed from the filtered image. In order to do this, area around the current pixel is examined, and if 80% of the area shows high intensity, these pixels are eliminated. On the other hand, if the area includes high intensity pixels and at least 20% of that area overlaps with vessels, those pixels are not eliminated. It is because of the fact that the current pixel with high intensity is next to a vessel in this case. Then, small vessel fragments and noisy structures, and unexpected high-low intensity areas are also removed from the filtered image. After that, a horizontal histogram of the filtered image and a vertical histogram of the strip around the maximum value of horizontal histogram are calculated. The maximum values in two histograms represent vertical and horizontal positions of the OD.

In some cases, the calculated middle point of the OD may slightly shift in vertical or horizontal direction from the real middle point. In these cases, high intensity values of the OD area are used for correcting the found location. The highest average intensity value (I.V.) of the several pixels in the determined area is used to determine the middle point of the OD. In order to do this, a simple intensity averaging method is applied for each neighboring pixels around the previously determined middle point of the OD. Hence, the pixel with maximum average intensity value in the neighboring area (15×15 pixels) is determined as the corrected middle point of the OD.

The histogram of vertical strip around OD as illustrated in Fig. 6 is only considered to calculate the horizontal position of OD. If there is some degeneration around the OD, the result may be a misdetection. To reduce the misdetection rate, a threshold technique is used. Therefore, histograms are calculated by considering only pixels with intensity values in a determined interval, which is from 30 to 170. Hence, normal OD area intensity distribution and vessels are considered rather than the intensity distribution of degenerations.

3.1.3. *Elimination of the OD area*

In the application, it is experimented that the OD area may also be segmented as DR lesion. Therefore, the OD area should be eliminated from the final segmented image. If the OD area is not eliminated, degeneration cannot be measured correctly. The OD area may be determined automatically or chosen manually by user. Then, if there are incorrectly segmented pixels around the OD as given in Fig. 8, these pixels are eliminated from the final segmented image by considering the average diameter of the OD. If consecutive images taken from the same patient on previous occasions are compared, elimination of OD area may not be necessary. In this kind of cases, only the differences between the degenerations on the sequential images are measured since the OD area is the same on all consecutive images for the same patient.

3.1.4. *Vessel elimination in retinal fundus images*

In the literature, many methods have been employed for detecting and segmenting vessels in retinal images [11,29,33,35,37] and X-ray angiograms [51,46]. These methods may also be used in segmentation of DR lesions. Retinal fundus images consist of wide range of vessel structures such as capillary, short, narrow, large and long vessels, and bleeding areas. The bleeding areas such as MAs and HEMs are early stages of the DR. If these structures are not eliminated correctly, they could be accounted as DR. Therefore, these areas should be eliminated to increase the accuracy of final segmentation of hard exudates and cotton wool spots. As a similar approach the automatic segmentation method developed for segmentation of ARMD exploits the vessel elimination technique [4,9]. The vessels around healthy regions mostly have relatively lower intensities than the pixels around them and these low intensity parts should also be segmented as healthy textures not to be considered unhealthy. A simple method is employed to eliminate these regions. This method examines the intensity value of each pixel on the image. If the intensity of a pixel is within the expected interval relative to the extended background image, it is considered to be on a blood vessel and set as healthy texture, otherwise the pixel is considered unhealthy. In this application, the interval dynamically changes according to the extended background image, which means that it is arranged according to the changing intensity values across the whole image. In other words, the threshold values of the interval dynamically change according to the intensity value of each pixel of the extended background image. As a result, all vessel structures and bleeding areas such as MAs and HEMs are eliminated for segmenting hard exudates and cotton wool spots successfully. On the other hand, MAs and HEMs have low intensity values similar to the vessel structure. In the application, these areas should be separated from segmented vessel structures. In this study, the vessels are first segmented by using the techniques in [46], which results in separation of small size MAs and large HEMs from the vessel structure. This part of the work is still in need of further improvements to increase the success.

3.2. *Segmentation methods for bright DR lesions*

In the literature, several direct methods are employed for segmenting and screening DR in retinal images [42,16,30]. The drawbacks of the current methods are mentioned in Section 1. In this paper, several inverse techniques are introduced for segmenting DR lesions in retinal images. These are region growing, region growing with background correction and adaptive region growing techniques with background correction. In region growing approach, simply several seed pixels are chosen, and then similar pixels are searched around the seed pixels. The second method adapts the similarity con-

Please cite this article in press as: C. Köse, et al., Simple methods for segmentation and measurement of diabetic retinopathy lesions in retinal fundus images, Comput. Methods Programs Biomed. (2011), doi:10.1016/j.cmpb.2011.06.007

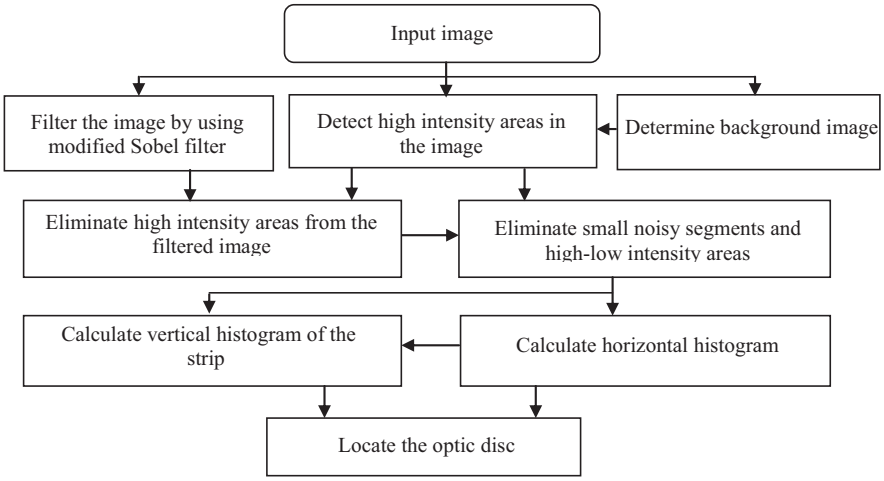

Fig. 7 – Locating the OD.

strains according to the background image. The last method, adaptive region growing method, adapts itself to the background and local intensity changes for a better segmentation. In this method, the threshold value is set experimentally according to the training data set that comprises mostly images with different sizes and kinds of lesions in order to be able to calculate a correct threshold. The test results show that the method works fine and little or no adjustments would be required in case the application is tested on a new data set.

3.2.1. *The inverse segmentation approach for segmentation of DR lesions*

In this study, we addressed a simple inverse segmentation approach for measuring the DR lesions in retinal images based on the techniques proposed in [4], and used in [9]. The inverse segmentation approach is based on the fact that the texture of unhealthy areas of retinal images is quite irregular and varies from eye to eye. In other words, unhealthy textures of retinal images differ quite dramatically in terms of size and texture according to our experiments. On the other hand, healthy tex-

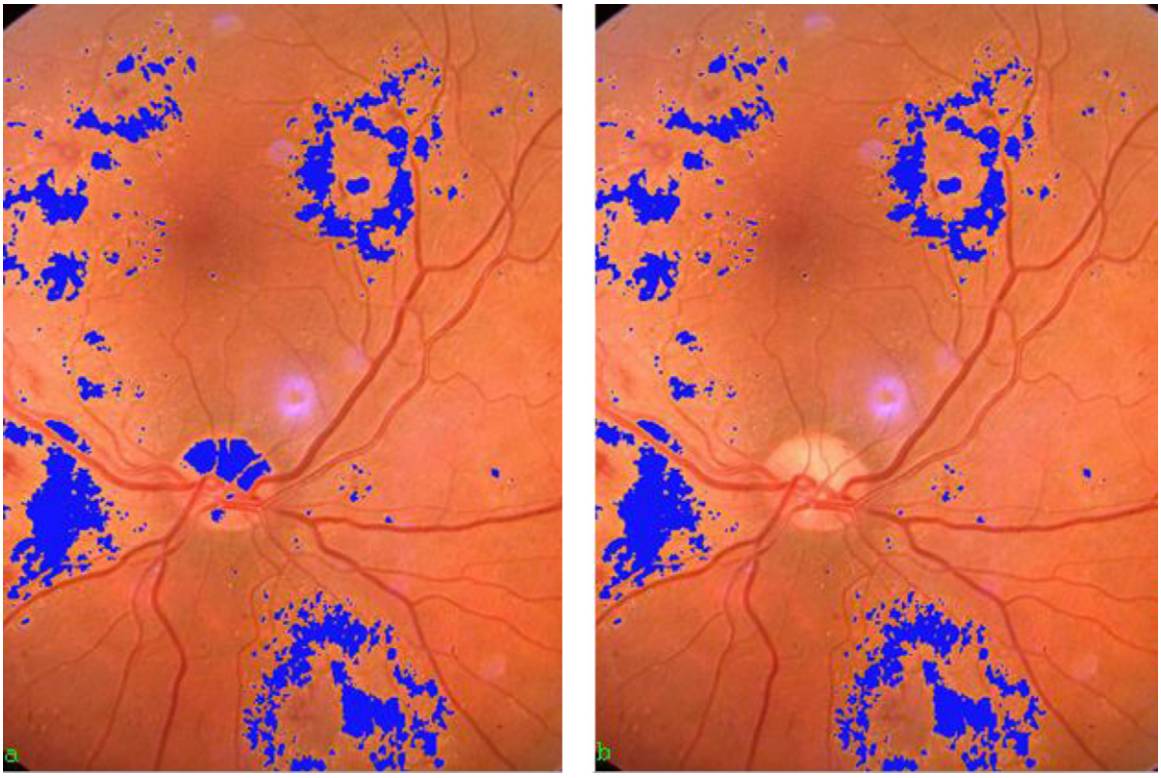

Fig. 8 – (a) A mis-segmented pixels around the optic disk area and (b) pixels eliminated around the optic disk.

Please cite this article in press as: C. Köse, et al., Simple methods for segmentation and measurement of diabetic retinopathy lesions in retinal fundus images, Comput. Methods Programs Biomed. (2011), doi:10.1016/j.cmpb.2011.06.007

tures of the retinal images do not vary that much. Considering the varying image conditions, lack of adaptive capabilities of the direct methods may result in poor segmentation. In this study, the simple inverse segmentation method is employed since it generates more accurate results than other direct segmentation methods.

In the application, the healthy areas of a retinal image are first segmented by employing the inverse segmentation method. Thus, unhealthy regions of the image are determined based on the healthy areas. In order to do this, in the last step of the process, the inverse of segmented image is taken to generate the targeted segmentation result shown in Fig. 9.

3.2.2. Region growing method

In the previous application, a simple region growing method is employed to segment ARMD in retinal fundus images [9]. In that study, it was seen that the method successfully segments the degeneration in macular area. In that application, the seed pixels are also chosen from the macular area and then the region growing method is applied to segment healthy regions in the macula according to Eq. (5). The region growing technique uses the average intensity and standard deviation to segment images. Each seed pixel is compared with the neighboring pixels. If the difference between the seed and neighboring pixels is in the interval as expressed in Eq. (5), the pixel is segmented as healthy. Fig. 9(b) shows the segmentation results of the region growing method. It is seen from the figure that the region growing method is quite successful in the macular region but if background intensity changes dramatically across the image, the method may fail in segmentation of the whole retinal image. Thus, some parts of the image such as macula may be segmented quite successfully but the other parts may not be segmented that successfully.

$$Im\ g(i,j)\_seg = \begin{cases} \text{Healthy} & \text{if } |Im\,g\_org(i,j) - \mu| \le \Delta \\ \text{Unhealthy} & \text{Otherwise or vessel} \end{cases} \quad (5)$$

where $\mathrm{Im}\,g(i,j)\_seg$ is the segmentation results, $\mathrm{Im}\,g\_org(i,j)$ represents the intensity of the current pixel, μ represents the average of the currently segmented pixels and Δ represents the reference threshold and is set to 9.

3.2.3. Region growing method with background correction

In segmentation of ARMD, the macular area is selected as the region of interest. On the other hand, DR lesions may spread across the whole retinal image and more efficient techniques may be needed to segment the lesions. Therefore, the features of the background image are exploited to enhance the region growing technique. Then, Eq. (6) is used to segment the whole retinal image. Intensity changes are tolerated across the image, but over segmentation is encountered in some cases as shown in Fig. 9(c). This region growing approach with background correction method adapts itself to changes in background and achieves better segmentation compared to the first approach. If the difference between background image and the average of the currently segmented pixels increases unexpectedly, the segmentation approach would fail especially around the vessels. To enhance the segmentation, the difference is tolerated by employing an adaptive region growing method with background correction, which is explained in the following sections.

$$Img(i,j)\_seg = \begin{cases} \text{Healthy} & \text{if } |Im\,g\_org(i,j) - \mu + \alpha_{l,u}[Im\ g\_bgnd(i,j) - \mu]| \le \Delta \\ \text{Unhealthy} & \text{Otherwise or vessel} \end{cases} \quad (6)$$

where $\mathrm{Im}\,g_{bgnd}(i,j)$ is the background image and α is background toleration constant. $\mathrm{Im}\,g\_org(i,j) - \mu + \alpha_{l,u}[\mathrm{Im}\,g\_bgnd(i,j) - \mu]| \le \Delta$ is expressed and used as $-\Delta + \mu - \alpha_l[\mathrm{Im}\,g\_bgnd(i,j) - \mu] < \mathrm{Im}\,g\_org(i,j) < \Delta + \mu - \alpha_u[\mathrm{Im}\,g\_bgnd(i,j) - \mu]$. Thus, $(\alpha_{l,u})$, the lower and upper values, are constants. They were selected based on training data set, and set to 0.95 and 0.50, respectively. These values are set experimentally.

3.2.4. Adaptive region growing method with background correction

As seen from the figures, DR degenerations may spread across the whole retinal image and average intensity may also change dramatically across the image. These changes should be tolerated by the automatic segmentation method to segment the whole image successfully. Therefore, the difference between the background image and the average of the currently segmented pixels is efficiently tolerated by using Eq. (7). Hence, intensity changes across the image are tolerated and DR lesions across the retinal images are successfully segmented. Results show that this automatic region growing approach dynamically adapts itself to the changing image conditions and quite successfully segment all DR lesions across the retinal image without any user involvement. A sample segmented image is shown in Fig. 9(d). In the figure, a specific example is given to emphasize the difference between the proposed methods. On the other hand, better segmentation results may be generated by using specific parameters for each image. In general, the methods generate similar segmentation results as given in Section 5. The performance of the first approach depends on the seed pixels. The last method, the adaptive region growing method with background correction, generates the best segmentation results. The parameters used in the methods are applied in generation of the results. Our results show that the adaptive region growing method with background correction is the best method achieving very good segmentation performance in general.

$$Im\ g(i,j)\_seg = \begin{cases} \text{Healthy} & \text{if } |Im\,g\_org(i,j) - \mu + \alpha_{l,u}[Im\ g\_bgnd(i,j) - \mu] - \beta[\mu - Im\ g\_org(i,j)]| \le \Delta \\ \text{Unhealthy} & \text{Otherwise or vessel} \end{cases} \quad (7)$$

where β, representing average correction constant, is set to 0.5. The $\alpha_{l,u}$ value is set as in Section 3.2.3. This value is also experimentally set for the best segmentation result.

3.2.5. Bayesian approach (BA) for segmentation of DR

In previous section, adaptive region growing methods with background correction are introduced for segmenting DR in retinal fundus images. In this section, Naïve Bayes method is employed for segmentation of DR. Naïve Bayes, based on

Please cite this article in press as: C. Köse, et al., Simple methods for segmentation and measurement of diabetic retinopathy lesions in retinal fundus images, Comput. Methods Programs Biomed. (2011), doi:10.1016/j.cmpb.2011.06.007

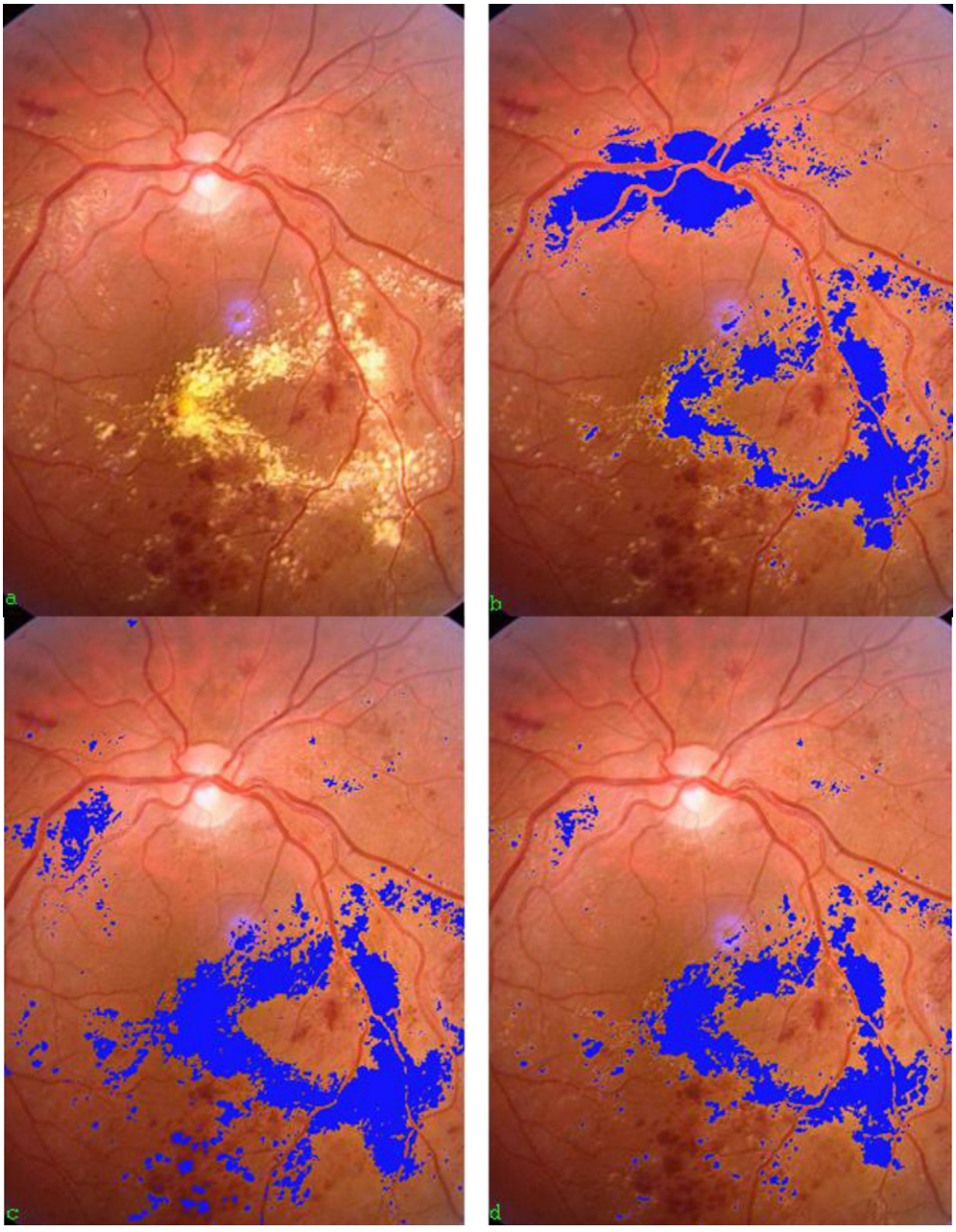

Fig. 9 – (a) An original image, (b) segmented image by using the region growing method, (c) the region growing method with background correction and (d) the adaptive region growing method with background correction.

Bayesian theorem, is a well known technique using high dimensional input space. Naïve Bayes classifiers can also use an arbitrary number of independent variables whether they are continuous or categorical. In this application, Naïve Bayes method exploits the futures of colors and intensity of textures or degenerations for segmentation of DR. Eq. (8) is employed to segment the degenerations in the retinal fundus images.

$$Im\ g(i,j)\_seg\{C(f_1,\ldots,f_d)\} = \max_k \{p(C_n)\prod_{k=1}^{d} p(x_k|C_n)\} \quad (8)$$

where Im $g(i, j)\_seg$ is the segmentation result. f, k, n and C represent the features, feature indices and class, and class variable, respectively. d is the number of features. $p(C_n)$ and $p(x_k|C_n)$ stand for the class priority and independent probability distributions, respectively. The classification result $C(f_1, \ldots, f_n)$ is also set as the segmentation result of the current pixel.

Practically, Naïve Bayes method reduces the high-dimensional density estimation task to one-dimensional kernel density estimation. In this application, intensity, RGB color components, the differences between colors and luminance, average and standard deviations of pixels intensities and colors, and sizes and dimensions of degenerations were

Please cite this article in press as: C. Köse, et al., Simple methods for segmentation and measurement of diabetic retinopathy lesions in retinal fundus images, Comput. Methods Programs Biomed. (2011), doi:10.1016/j.cmpb.2011.06.007

Fig. 10 – An original image (a), segmented image by using Bayesian method (b) and adaptive region growing method with background correction (c).

used as features of the lesions and other regions in detection of lesions. Probability distribution for each feature on the training data set is computed for the lesions and other areas. For the classification, probabilities for each pixel are calculated using the probability distributions. Finally, the resulting class probability and the calculated probabilities for each class are multiplied to classify the pixel with maximum value. In Fig. 10, segmentation results of Bayesian and adaptive region growing with background correction methods are given. The most important advantages of the adaptive region growing with background correction method are simplicity and efficiency in the segmentation. If the images are carefully examined, Bayesian method shows over segmentation in some part of image and under segmentation in some other parts. Considering the segmentation of hard exudates, as given in the figure, Bayesian approaches generate mis-segmented small fragments, whereas the adaptive region growing with background correction method segments the target area more smoothly. Especially, the fragments may spread across the whole image. On the other hand, the adaptive region growing with background correction method shows quite efficient and consistent segmentation performance all across the image.

3.3. *Segmentation method for dark DR lesions*

In this paper, we have introduced a simple approach for segmenting dark DR lesions in retinal images. The method is applied to segment the region with lower intensity value than the background image intensity value. Hence, the low intensity region consists of vessels and dark lesions. Then, the vessel segmentation method [46] is employed to remove the vessels. The remaining after the vessel segmentation are the dark lesions and they are set as degenerated area. In other words, the extended background image almost follows the healthy retinal texture except vessels and OD. Therefore, a threshold value is set just under the intensity value of the background image. So, the pixels with lower intensity than the threshold value are set as degenerated area after the vessel elimination or remove operation by using the vessel segmentation method. These pixels are given in yellow in the resulting segmented image.

4. Measurements of DR and evaluation of course of the disease

In the medical departments, ophthalmologists have to deal with large amount of retinal images. Thus, an automatic segmentation and measurement method may enable the ophthalmologists to analyze the images more rapidly. Proposed method generates a complete segmentation of lesions in a retinal fundus image, and then it enables the user to measure the area of DR lesions automatically. As an example a manually segmented DR on image and an automatically segmented DR on the same image are given in Fig. 11(b) and (c), respectively.

4.1. *Measuring and comparing the segmentation results*

As mentioned before, experiments show that manual segmentation and measurement of DR lesions are quite difficult, and user may easily make mistakes during the segmentation [1–3]. Quality of segmentation also changes depending on the quality of image and ability and experience of user. In this application, four metrics are applied to reveal the segmentation performance of application. First metric is shown as Eq. (9), which determines the segmentation accuracy;

$$\text{Accuracy} = \frac{Tn + Tp}{Tn + Tp + Fn + Fp} \tag{9}$$

where Tp, Tn, Fn and Fp stand for true positive, true negative, false negative and false positive, respectively.

$$\text{PPV} = \frac{Tp}{Tp + Fp} \tag{10}$$

Please cite this article in press as: C. Köse, et al., Simple methods for segmentation and measurement of diabetic retinopathy lesions in retinal fundus images, Comput. Methods Programs Biomed. (2011), doi:10.1016/j.cmpb.2011.06.007

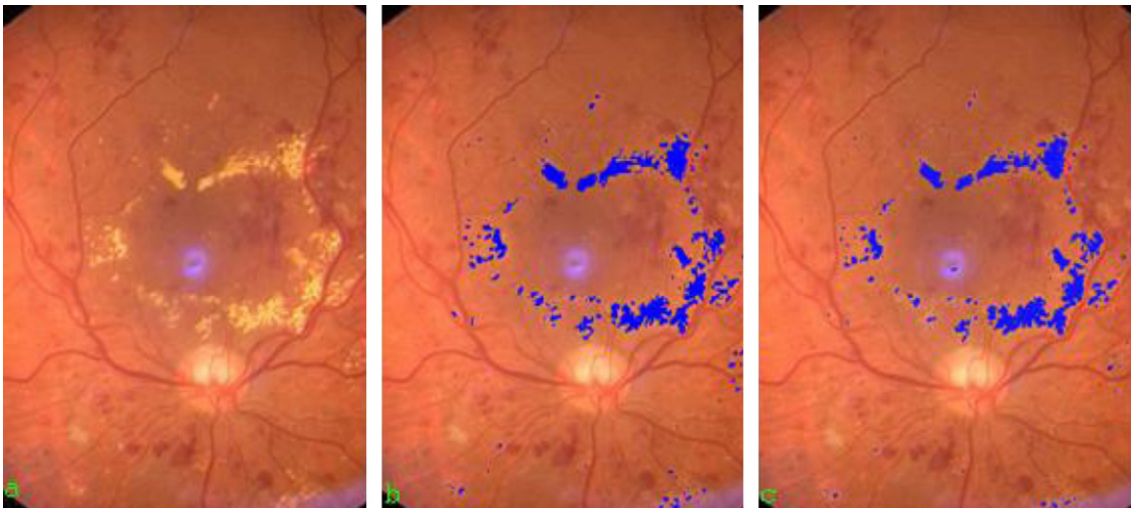

Fig. 11 – (a) An original image, (b) a manually and (c) automatically segmented image by using the inverse method.

The positive predictive value (PPV), sensitivity and specificity are also widely used statistical measurements to present the test results in more understandable form. The positive predictive value or precision rate is the proportion of the true positives to positive test results. The positive predictive value is determined by using Eq. (10).

$$\text{Sensitivity} = \frac{Tp}{Tp + Fn} \tag{11}$$

Other metrics are sensitivity and specificity. Sensitivity is the proportion of true positives correctly classified by the system. Specificity is the proportion of the true negatives correctly classified by the system. Sensitivity and specificity values are calculated by using Eqs. (11) and (12).

$$\text{Specificity} = \frac{Tn}{Tn + Fp} \tag{12}$$

Monitoring effectiveness of an applied medical treatment is important. Therefore, a simple comparison method is employed to measure recovery obtained by a medical treatment or negative changes of the disease. In this application, a simple method is employed to measure the size of DR lesions based on Eq. (13).

$$Deg\_Area = \sum_{i=1}^{M}\sum_{j=1}^{N}\{Pixel(i,j)\} \cdot seg \tag{13}$$

where *Deg_Area* is the degenerated area in retina. *Pixel*(i, j), representing the pixels in the area as degenerated, is set to 1, and *seg* represents segmentation results. In this application, *seg* is 1 for segmented pixels and 0 for other pixels.

Eq. (14) is used to measure the differences between segmented images taken at consecutive occasions.

$$Seg\_Diff = Deg\_Area(Im\ g\_1) - Deg\_Area(Im\ g\_2) \tag{14}$$

where *Seg_Diff* is the total difference between segmentation results of first "*Seg_Area*(Im *g*_1)" and second "*Seg_Area*(Im *g*_2)" images taken from the same patient taken at different occasions.

4.2. *Diagnosing the DR*

Automatic screening of the DR is preferable because it avoids inter/intra-observer variability and better suits for clinical studies and measurements [1,3,8,29,33]. In this application, region where DR lesions affected is determined by calculating the number of pixels segmented as unhealthy in the retinal image. If area of lesions is larger than a threshold value (an experimentally determined value), the DR is diagnosed as positive. Then, ophthalmologist may take the patient into further examination and apply proper medical management of DR.

4.3. *Data set used in evaluation of the application*

In this study, a total of 328 images with 760 × 570 pixels resolution in various qualities were used in evaluation of the developed system. The images were obtained from digital fundus camera situated at Department of Ophthalmology, at Faculty of Medicine, in Karadeniz Technical University. Different stages of the method employ different subsets of these images. Here, our experienced ophthalmologist manually marked all lesions in the images as images with hard exudates, cotton wool spots and MAs and HEMs. The marked areas were also considered in selection of ground truth data as the reference standard to compare our segmentation results. The employed subset on tests was constituted according to the classification done by Ophthalmologists. In tests, all of 328 images in data set including images with different kinds of degenerations and retinal illnesses such as DR, ARMD, optic nerve hypoplasia, glaucoma, and optic nerve pit were used to measure the general performance of the system in OD detection. A subset of the images, including 217 images, was also employed to test OD detection performance of the system in DR, ARMD and similar cases. Another subset, including 111 images, was also used to test OD detection performance of the system for only DR cases. Finally 62 images were used

Please cite this article in press as: C. Köse, et al., Simple methods for segmentation and measurement of diabetic retinopathy lesions in retinal fundus images, Comput. Methods Programs Biomed. (2011), doi:10.1016/j.cmpb.2011.06.007

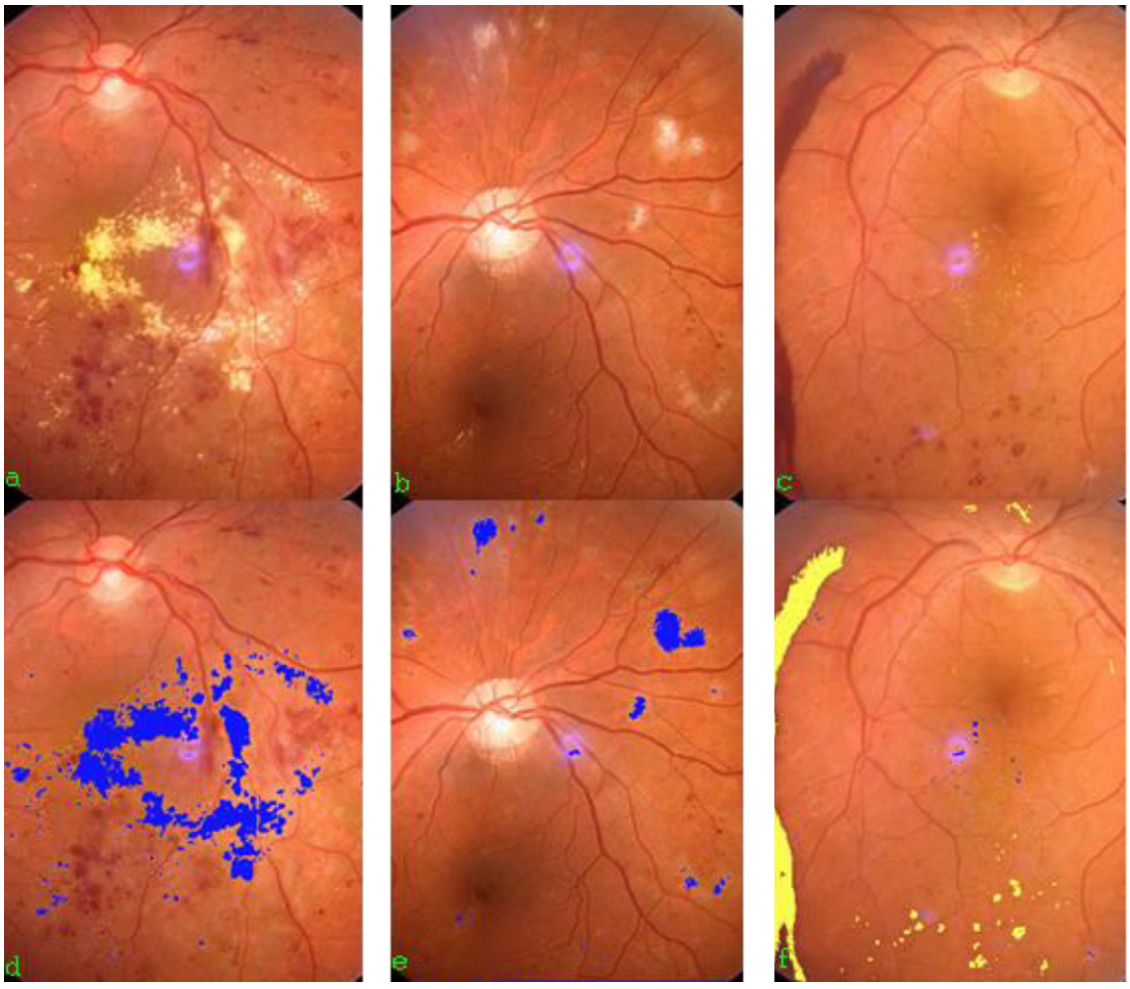

Fig. 12 – Original images with (a) hard exudates, (b) cotton wool spots, and (c) MAs and HEMs, and their segmentations (d–f) using proposed automatic method.

for segmenting, and measuring and evaluating the system in terms of segmentation capability on DR. A set of 12 and 50 images in different colors, brightness, and quality are used to train and test the system, respectively. Among the images in the data set, 12, 4, 2 and 3 of the test images in data set carry hard exudates, cotton wool spots, MAs and HEMs, respectively. Moreover 13 and 2 of the test images include the combinations of degenerations of hard exudates-MAs, and cotton wool spots-MAs, respectively. 11 and 1 of the test images include the combinations of degenerations of hard exudates–cotton wool spots–MAs, and cotton wool spots–MAs–HEMs, respectively. Only 2 images in the test data set carry all kind of degenerations.

Only 12 images were included in the training set since some images containing one or more type of lesions are quite adequate to tune threshold value of the system. For the training set, the parameters are tuned to obtain the best accuracy result which is 0.978. Then, the same values of the parameters are applied on test set to obtain the results in this study. Our experiments also show that the automatic system works fine and little adjustments are required to set the thresholds values. After training phase, the proposed methods are successfully tested on large number of images. The results show that the system adjusted with the threshold values successfully detects OD and segments DR automatically.

5. Results

In this study, an automatic method is implemented for segmenting and screening the DR in retinal fundus images. Experiments and measurements were performed on a PC with P4-3.2 GHz CPU and 1024 MB RAM. Fig. 12 shows three original retinal fundus images with hard exudates, cotton wool spots, MAs and HEMs, and their automatic segmentation results. In this application, the dark regions under the varying threshold (extended background image) are segmented as MAs and HEMs. In general, large areas can be considered as HEMs and small areas can be considered as MAs except for the vessel. These regions showing MAs and HEMs are segmented as yellow areas in Fig. 12(f).

In this study, most of the images with hard exudates and cotton wool spots, and some images with MAs and HEMs, are used in examination of automatic segmentation method with the background image extraction. Segmentation of MAs and HEMs was conducted by employing blood vessel segmenta-

Please cite this article in press as: C. Köse, et al., Simple methods for segmentation and measurement of diabetic retinopathy lesions in retinal fundus images, Comput. Methods Programs Biomed. (2011), doi:10.1016/j.cmpb.2011.06.007

Table 1 – Distribution of degenerations or lesions in retinal images.

	DR lesions	
	Number of images	In %
Degeneration spreads around macula	22	19.8
Degeneration spreads in whole image	89	80.2
Total number of images	111	100

tion method presented in [46]. Hence, more experiments are needed to be carried out for the segmentations of vessels in retinal images with MAs and HEMs. Therefore, our results mostly show the performance of the automatic method on the hard exudates and cotton wool spots. Thus, the test results also show that our method overcame most of the limitations of previous methods.

In order to present the performance of our method, the system was tested on images with different kinds and sizes of degenerations such as DR, and small, medium and large degenerations. The important point is to locate the ODs in many different and complex cases. In addition to these, morphologies and properties of the degenerations show similarities. Therefore, all images are included in the measurement of the performance of the system in OD localization. On the other hand, only images with DR are used in measurement of the segmentation performance.

To show the differences in the segmentation of DR, distributions of the degenerations in retinal images are also obtained and presented in Table 1. It is seen in the table that most of the diabetic lesions are spread across the whole retinal image.

In the optic disk detection, most of the results are taken for the images with DR, age-related degenerations and without degeneration. Results for detecting OD and eliminating OD area are given in Table 2. These results show about 98% of the OD on the images with no, little or medium degenerations, are detected successfully. On the other hand, about 93% of the OD in the images with the large degeneration is detected successfully. Thus, the general performance of the system is about 98%. In overall performance column, two different results are given for the cases that the number of roughly located ODs and ODs located by correction are not the same. The intensity averaging method increases the precise OD detection performance except one of the image with medium degeneration.

Our experiments show that the performance of the system varies related to the size of the degenerations. Therefore, results are generated for small, medium and large sizes of degenerations. Sizes of the small, medium and large degenerations are classified between 0 and 1000, 1000 and 15,000, and >15,000 pixels, respectively.

Results in Table 3 show that ODs in the images with little DR lesions are detected successfully. About 98% of the ODs on the images with medium degenerations are detected successfully. On the other hand, about 92% of the ODs in the images with large degenerations are detected successfully and the general performance of the system is about 96%.

For the segmentation, all of the test images with DR, given in Table 3, are processed in 35.89 min using the system. The average processing time of one image is found to be 19.4 s. In this application, the threshold is established according to experiments of ophthalmologists based on many clinical tests and experiments. In most cases, experiments show that the segmentation method works fine and little or no adjustments are required to correct the outline of the degenerated area. The processing time shows that the system is quite promising to process large number of image set.

General performance of the system in detecting OD in retinal images is given in Table 4. These results show that over 92% of the OD in retinal images with large degeneration is located correctly. Overall performance of the system is over 97%. The term precisely located on the top of the columns in Table 4 means that the centers of ODs are determined correctly as suggested by the ophthalmologist. On the other hand, roughly located ODs is used for OD detections. OD is found not in the center but somewhere in its covering area. Wrongly located ODs indicate that OD was not able to be detected but it may be close to the OD area. The intensity averaging method increases the OD detection performance on all images except for one of the image with medium degeneration in data set.

A comparison between manual method, Bayesian and region growing segmentation methods for DR measurement is given in Table 5. MS, BSM, NOS, PPV, RGS, RGMBC and ARGMBC stand for manual segmentation, Bayesian segmentation method, not-overlapping segmentations, positive predictive value, region growing segmentation, region growing method with background correction and adaptive region growing method with background correction, respectively. In this table, first three lines show performances of the approaches applied on images with small, medium and large scale degenerations. Average performances of Bayesian methods and region growing methods as PPV are given in the last line of the table which are about 0.875 and 0.918, respectively. Our experiments state that Bayesian methods show quite varying performance in segmentation of DR such as under and over segmentation. Even in some cases re-evaluation of training samples may be required to get a better segmentation results. On the other hand, inverse region growing methods show quite consistent and effective performances in all cases. In general, threshold values can be set and tuned easily to obtain a better segmentation results. Considering BSM, choosing the best training samples and eliminating the bad ones are quite problematic, and segmentation results cannot be estimated regarding the samples used in the training.

Performance of the proposed method and RGMBC on the same test images is given in Table 6. In the table, first three lines show the performance of the approaches applied on images with small, medium and large scale of degenerations. Average performance of RGMBC is given in the last line of the table, which is 0.901. In some cases, the system presents a relatively low performance for images with small and scattered degenerations. In those cases, a threshold value such as proper segmentation size may be chosen for a better segmentation and distribution can be taken as parameter. In such cases, the adaptive region growing approach with background correction is employed for further enhancement. The result of this enhancement is given in the following paragraph. Average performance of ARGMBC is also given in the last line of the table, which is 0.925. The results prove that manual and pro-

Please cite this article in press as: C. Köse, et al., Simple methods for segmentation and measurement of diabetic retinopathy lesions in retinal fundus images, Comput. Methods Programs Biomed. (2011), doi:10.1016/j.cmpb.2011.06.007

Table 2 – Locating ODs with/without some degree of degenerations.

	Number of images	Precisely located ODs	Roughly located ODs	Wrongly located ODs	Corrected by I.V.	Overall performance (in %)
Images without degenerations	42	40	1	1	1	97.6
Images with small degenerations	61	52	8	1	8	98.3
Images with medium degenerations	72	58	14	-	13	100
Images with large degenerations	42	30	9	3	9	92.9
Overall performance	217	180	32	5	31	97.7

Table 3 – Locating ODs with DR lesions.

	Number of images	Precisely located ODs	Roughly located ODs	Wrongly located ODs	Corrected by I.V.	Overall performance (in %)
Images with small degenerations	27	20	7	–	7	100
Images with medium degenerations	48	37	9	2	10	97.9
Images with large degenerations	36	24	7	5	9	91.7
Overall performance	111	81	23	7	26	96.4

Table 4 – General performance of the system in locating ODs.

	Number of images	Precisely located ODs	Roughly located ODs	Wrongly located ODs	Corrected by I.V.	Overall performance (in %)
Images without degenerations	42	40	1	1	1	97.6
Images with small degenerations	88	72	15	1	15	98.7
Images with medium degenerations	120	95	23	2	24	99.2
Images with large degenerations	78	54	16	8	18	92.3
Overall performance	328	261	55	12	58	97.3

Table 5 – A comparison of the manual, Bayesian and region growing methods.

	MS	Bayesian method			Region growing method		
		BSM	NOS	PPV	RGS	NOS	PPV
Image with small degenerations	625	721	96	0.877	672	47	0.943
Image with medium degenerations	3665	4084	419	0.892	3893	228	0.948
Image with large degenerations	33154	37325	4171	0.881	29867	3287	0.907
Average for 50 images	8334	9438	1104	0.875	9195	861	0.918

posed automatic methods achieve quite similar performances in measuring the DR lesion in retinal images. Besides, our automatic segmentation method can reduce the processing time significantly compared to the manual method.

According to our experiments, processing an image automatically takes less than 15 s, which takes up to 1 h when manual method is used. Segmentation results of ARGMBC are presented in Table 6, a t significance test is conducted for a quantitative assessment. Thus, two tailed P values are calculated as 0.7941 while the intermediate values are calculated as $t = 0.2624$, $df = 49$, and standard error of the difference is 242.5. This result shows that the difference between manual and automatic segmentations is statistically insignificant in 95% of confidence.

Performances of the automatic segmentation method for hard exudates, cotton wool spots, and MAs and HEMs are given in Table 7. The system provides quite good segmentation performances for hard exudates and cotton wool spots, and segmentation results of the MAs and HEMs are also encouraging. Average performances are given in the last line of the table which are about 0.98 for hard exudates and cotton wool spots and about 0.97 for MAs and HEMs. The results could still be improved by using more proper vessels segmentation method which is still under examination.

Table 6 – A comparison of the manual, RGMBC and ARGMBC.

	MS	RGMBC			ARGMBC		
		RGMBC	NOS	PPV	ARGMBC	NOS	PPV
Image with small degenerations	625	682	57	0.922	572	53	0.921
Image with medium degenerations	3665	3876	211	0.950	3506	159	0.956
Image with large degenerations	33154	36415	3261	0.918	31915	1239	0.963
Average for 50 images	8334	9235	901	0.901	7767	567	0.925

Please cite this article in press as: C. Köse, et al., Simple methods for segmentation and measurement of diabetic retinopathy lesions in retinal fundus images, Comput. Methods Programs Biomed. (2011), doi:10.1016/j.cmpb.2011.06.007

Table 7 – A comparison of performances of the automatic method on the hard exudates, cotton wool spots, and micro-aneurysms and HEMs.

	Hard exudates		Cotton wool spots		MAs		HEMs	
	PPV	Accuracy	PPV	Accuracy	PPV	Accuracy	PPV	Accuracy
Image with small degenerations	0.915	0.999	0.926	0.999	0.801	0.999	0.821	0.999
Image with medium degenerations	0.957	0.998	0.934	0.998	0.878	0.998	0.895	0.995
Image with large degenerations	0.964	0.989	0.930	0.987	0.893	0.984	0.835	0.965
Average performance	0.951	0.988	0.927	0.986	0.867	0.982	0.846	0.971

Table 8 – A comparison of performances of the automatic method as sensitivity and specificity measures.

	Hard exudates		Cotton wool spots		MAs		HEMs	
	Sensitivity	Specificity	Sensitivity	Specificity	Sensitivity	Specificity	Sensitivity	Specificity
Image without degenerations	–	0.999	–	0.999	–	0.999	–	0.999
Image with small degenerations	0.979	0.999	0.981	0.999	0.927	0.999	0.932	0.999
Image with medium degenerations	0.984	0.999	0.980	0.999	0.961	0.999	0.963	0.999
Image with large degenerations	0.988	0.996	0.981	0.997	0.965	0.993	0.937	0.991
Average performance	0.981	0.998	0.976	0.996	0.951	0.993	0.932	0.983

Lastly, to evaluate false positives and negatives, the performances of the segmentation method for hard exudates, cotton wool spots, and MAs and HEMs are measured as sensitivity and specificity, and their results are given in Table 8. In all test scenarios throughout the paper, the same threshold value and parameter are used to generate comparable and consistent results. Thus, a little bit over and under segmentations are encountered in some cases. But the proposed method is still quite efficient in segmentation of DR. In the application, the same threshold values may not be best for all images, and better segmentation result may be generated using different threshold values for different images, which also results in minimum over and under segmentations. In the table, the sensitivity values for the image without degeneration are not calculated because zero true positive pixels are suggested for those images. Average performances as sensitivity and specificity values are given in the last line of the table which are over 0.97 for hard exudates and cotton wool spots, and over 0.93 for MAs and HEMs.

In the literature, several methods are employed for segmenting DR in retinal fundus images [2,16,19,21,30,42]. In our study, an automatic segmentation approach is implemented and compared with the proposed method in [18]. The performance of the method tested on our images with hard exudates is about 90%, which is less than our overall success, which is 95%. A comparison of the segmentation results is given in Fig. 13. While the fuzzy art neural network and Bayesian methods under-segment or over-segment some pixels as shown in the figure, the proposed method with background correction segments the image quite consistently. The fuzzy art method may be applied to segment bright lesions but it is not that much suitable for segmenting dark lesions. Since the fuzzy art network method is not applicable for all lesions, the results are not comparable with ours. On the other hand, even though we gave this comparison, it should be stated that this comparison may not be fair because our implementation of their method may not cover all the details since the published paper describing the method may not give all the details. Most of the

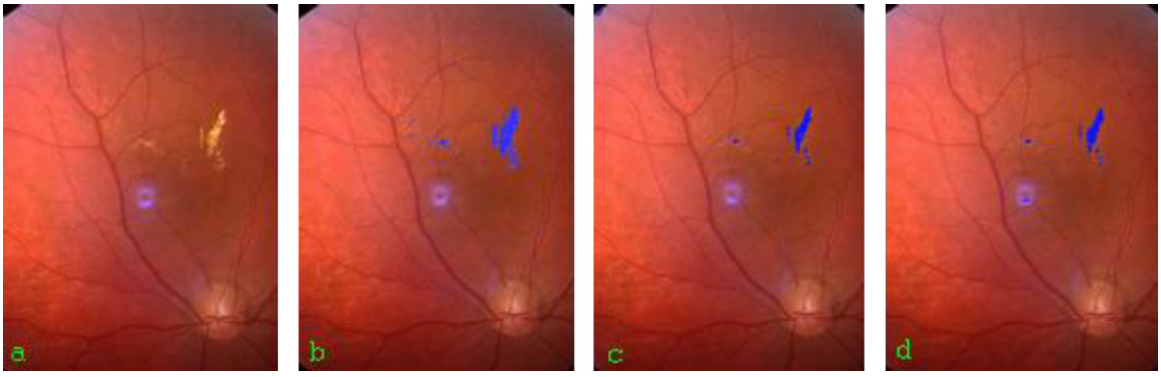

Fig. 13 – An original image (a), segmented image by using Bayesian method (b), fuzzy art neural network method (c), and our automatic method (d).

Please cite this article in press as: C. Köse, et al., Simple methods for segmentation and measurement of diabetic retinopathy lesions in retinal fundus images, Comput. Methods Programs Biomed. (2011), doi:10.1016/j.cmpb.2011.06.007

previous methods are applied to segment hard exudates and cotton wool spots, but they are not successful in the segmentation of MAs and HEMs. On the other hand, in this study a fully automatic method is realized for segmenting all of the degenerations including MAs and HEMs in the retinal fundus images.

Segmentation and measurement accuracies of three approaches were determined by comparing the degenerated retinal areas segmented by the automated methods with those segmented manually. The difference between manual segmentation and automatic segmentation is called segmentation accuracy. Tables 5 and 6 summarize the performances of the inverse segmentation approaches. Checking the last lines of the tables, average performances of the Bayesian methods, the region growing methods, RGMBC, and the ARGMBC as PPV are 0.875, 0.918, 0.901 and 0.925, respectively. These results show that adaptive region growing methods with background correction provide the best performance among segmentation methods studied in the paper. The results prove that the most successful automated method could be quite useful for screening the DR in retinal fundus images.

6. Conclusion and future work

In the literature, several methods are employed for segmenting and screening DR and detecting ODs in retinal fundus images [2,11,13,16,19,21,30,45]. Among those, most of the methods proposed for segmenting hard exudates do not segment cotton wool spots, MAs and HEMs. These direct segmentation methods are more complex and expensive than our inverse method because the texture of unhealthy areas of retina is quite irregular. It should be stated that other methods also fail in segmentation of textures that have similar color with degenerations. But the inverse segmentation method is used in this study because it generates more accurate results than other direct segmentation methods for segmenting DR. Other methods provide various performances in segmentation of DR lesions and localization of the OD and the macula. The methods with proper user involvement provide about 90% of segmentation accuracy [2,8,10,16,18,19,25]. On the other hand, OD localization performances of these methods are also more or less around 95% [27,28,32,36].

In this study, we proposed an inverse automatic approach implemented for detecting and screening DR lesions in retinal fundus images, which is relatively faster. In order to do this, an adaptive region growing method with background correction for bright lesions and the background based method for dark lesions are addressed. The proposed method, evaluated on 50 retinal fundus images, allows higher segmentation accuracy than the other methods do. The complete analysis of a retinal image can be done in less than half of a minute without any user involvement. The method detects and localizes over 97% of the ODs and segments over 95% of DR lesions accurately. Therefore, the method provides a quite high segmentation and measurement accuracy. The method also measures how much the degeneration spread across the image compared to the previous conditions. This proposed approach has also the ability to remove blood vessels in the retinal images, and it also eliminates the OD area to measure lesions correctly. In addition to these, unlike most of the previous segmentation methods that are only applicable to one or two types of the DR lesions, our method segments all types of DR lesions.

Our experiments show that the methods proposed for segmentation of DR may also be applied to analyze other kind of degenerations in retinal images, which could be considered as a future work. Since the proposed system is relatively less successful in locating OD in retinal images with large degenerations, another future work would be the improvement of the performance of the system in locating OD in those kinds of images with large degenerations. There are also a few cases such as image lighting artifacts where our automatic method is able to achieve a relatively lower segmentation performance. In some cases, the image lighting artifacts may affect segmentation performance negatively, which could also be considered another problem of future tasks to be solved. More efficient vessel segmentation techniques may be employed for a better segmentation of MAs and HEMs, which can be considered as another future work. In some cases, DR lesions and high intensity areas such as OD may not be separated from each other. This may as well affect the segmentation results negatively. Fuzzy techniques as feature work may be useful in separation of these two regions. An OD location confirmation technique can also be considered as another future improvement to increase reliability of the method.

Conflict of interest

There is no conflict of proprietary, financial, professional or other personal interest with any person or organization regarding the material discussed in the manuscript.

Acknowledgements

The digital color fundus images were provided by Faculty of Medicine at Karadeniz Technical University. We extend our appreciation to the members of the faculty for providing us with valuable digitized images stored in their database.

REFERENCES

[1] M. Wilson, P. Soliz, S.C. Nemeth, Computer-aided methods for quantitative assessment of longitudinal changes in retinal images resenting with maculopathy, Medical Imaging 4681 (2002) 150–170.
[2] C.I. Sanchez, R. Hornero, M.I. Lopez, J. Poza, Retinal image analysis to detect and quantify lesions associated with diabetic retinopathy, in: Engineering in Medicine and Biology Society, 2004, IEMBS'04. 26th Annual International Conference of the IEEE, vol. 1, 2004, pp. 1624–1627.
[3] T. Smith, V. Sivagnanavel, J.K. Chan, et al., An inter-institutional comparative study of drusen segmentation and quantification using a digital technique of fundus background reconstruction, Investigative Ophthalmology & Visual Science 45 (2004), E-Abstract 2424.
[4] C. Köse, U. Şevik, O. Gençalioğlu, Automatic segmentation of age-related macular degeneration in retinal fundus images, Computers in Biology and Medicine 38 (2008) 611–619, doi:10.1016/j.compbiomed.2008.02.008.

[5] K. Rapantzikos, M. Zervakis, K. Balas, Detection and segmentation of drusen deposits on human retina: potential in the diagnosis of age-related macular degeneration, Medical Image Analysis 7 (2003) 95–108.
[6] T.J. Wolfensberger, P.A.M. Hamilton, Diabetic retinopathy – an historical review, Royal Swets & Zeitlinger, Seminar in Ophthalmology 16 (2001) 2–7.
[7] R.T. Smith, J.K. Chan, T. Nagasaki, et al., Automated detection of macular drusen using geometric background leveling and threshold selection, Archives of Ophthalmology 23 (2005) 200–206.
[8] T. Walter, J.C. Klein, P. Massin, A. Erginay, A contribution of image processing to the diagnosis of diabetic retinopathy – detection of exudates in color fundus images of the human retina, IEEE Transactions on Medical Imaging 21 (2002) 1236–1243.
[9] C. Köse, U. Şevik, O. Gençalioğlu, C. İkibaş, T. Kayıkçıoğlu, A statistical segmentation method for measuring age-related macular degeneration in retinal fundus images, Journal of Medical Systems 34 (2010) 1–10, doi:10.1007/s10916-008-9210-4.
[10] A. Sopharak, B. Uyyanonvara, S. Barman, et al., Automatic detection of diabetic retinopathy exudates from non-dilated retinal images using mathematical morphology methods, Computerized Medical Imaging and Graphics 32 (2009) 720–727.
[11] A.W. Reza, C. Eswaran, S. Hati, Diabetic retinopathy: a quadtree based blood vessel detection algorithm using RGB components in fundus images, Journal of Medical Systems 32 (2008) 147–155.
[12] M. Niemeijer, B. van Ginneken, S.R. Russell, et al., Automated detection and differentiation of drusen, exudates, and cotton-wool spots in digital color fundus photographs for diabetic retinopathy diagnosis, Investigative Ophthalmology & Visual Science 48 (2007) 2260–2267.
[13] M. Niemeijer, B. van Ginneken, M.J. Cree, A. Mizutani, G. Quellec, C.I. Sánchez, B. Zhang, R. Hornero, M. Lamard, C. Muramatsu, X. Wu, G. Cazuguel, J. You, A. Mayo, Q. Li, Y. Hatanaka, B. Cochener, C. Roux, F. Karray, M. García, H. Fujita, M.D. Abràmoff, Retinopathy online challenge: automatic detection of microaneurysms in digital color fundus photographs, IEEE Transactions on Medical Imaging, IEEE Publishing 29 (2010) 185–195.
[14] T. Walter, P. Massin, A. Erginay, R. Ordonez, C. Jeulin, J.-C. Klein, Automatic detection of microaneurysms in color fundus images, Medical Image Analysis 112 (2007) 555–566.
[15] K. Estabridis, R.J.P. de Figueiredo, Automatic detection and diagnosis of diabetic retinopathy, in: Image Processing, 2007. ICIP 2007. IEEE International Conference, vol. 2, 2007, pp. 445–448.
[16] S.S. Lee, M. Rajeswari, D. Ramachandram, B. Shaharuddin, Screening of diabetic retinopathy – automatic segmentation of optic disc in colour fundus images, in: Proceedings of DFMA 2006: The 2nd International Conference on Distributed Frameworks for Multimedia Applications, 2006, pp. 37–43.
[17] M. García, C.I. Sánchez, J. Poza, M.I. López, R. Hornero, Detection of hard exudates in retinal images using a radial basis function classifier, Annals of Biomedical Engineering (Springer) 37 (2009) 1448–1463.
[18] C. Jayakumari, T. Santhanam, Detection of hard exudates for diabetic retinopathy using contextual clustering and fuzzy art neural network, Asian Journal of Information Technology 6 (2008) 842–846.
[19] S.S. Basha, K.S. Prasad, Automatic detection of hard exudates in diabetic retinopathy using morphological segmentation and fuzzy logic, IJCSNS International Journal of Computer Science and Network Security 8 (2008) 211–218.
[20] H. Nguyen, A. Roychoudhry, A. Shannon, Classification of diabetic retinopathy lesion from stereoscopic fundus images, in: Engineering in Medicine and Biology Society, 1997. Proceedings of the 19th Annual International Conference of the IEEE, vol. 1, 1997, pp. 426–428.
[21] M.S. Chen, C.S. Kao, C.C. Fu, C.J. Chen, T.Y. Tai, Incidence and progression of diabetic retinopathy among non-insulin-dependent diabetic subjects: a 4-year follow-up, International Journal of Epidemiology 24 (1995) 787–795.
[22] R. Sivakumar, G. Ravindran, M. Muthayya, S. Lakshminarayanan, C.U. Velmurughendran, Diabetic Retinopathy Classification, in: TENCON 2003. Conference on Convergent Technologies for Asia-Pacific Region, vol. 1, 2003, pp. 205–208.
[23] M. García, C.I. Sánchez, M.I. López, D. Abásolo, R. Hornero, Neural network based detection of hard exudates in retinal images, Computer Methods and Programs in Biomedicine (Elsevier) 93 (2009) 9–19.
[24] G. Quellec, M. Lamard, P.M. Josselin, G. Cazugel, B. Cochener, C. Roux, Optimal wavelet transform for the detection of microaneurysms in retina photographs, IEEE Transactions on Medical Imaging 27 (2008) 1230–1241.
[25] C. Agurto, V. Murray, E. Barriga, et al., Multiscale AM–FM methods for diabetic retinopathy lesion detection, IEEE Transactions on Medical Imaging 29 (2010) 502–512.
[26] D. Satyarthi, B.A.N. Raju, S. Dandapat, Detection of diabetic retinopathy in fundus images using vector quantization technique, in: 2006 Annual India Conference (IEEE INDICON 2006), 2006, pp. 1–4.
[27] C. Sinthanayothin, J.F. Boyce, H.L. Cook, T.H. Williamson, Automated location of the optic disk, fovea, and retinal blood vessels from digital colour fundus images, British Journal of Ophthalmology 83 (1999) 902–910.
[28] H. Li, O. Chutatape, Automatic location of optic disk in retinal images, Proc. IEEE-ICIP 2 (2001) 837–840.
[29] O. Chutatape, L. Zheng, S.M. Krishnan, Retinal blood vessel detection and tracking by matched Gaussian and kalman filters. A tutorial review, in: Proc. 20th IEEE Conf. on Engineering in Medicine and Biology Society, 1998, pp. 3144–3149.
[30] H. Narasimha-Iyer, A. Can, B. Roysam, C.V. Stewart, H.L. Tanenbaum, A. Majerovics, H. Singh, Robust detection and classification of longitudinal changes in color retinal fundus images for monitoring diabetic retinopathy, IEEE Transaction on Biomedical Engineering 53 (2006) 1084–1098.
[31] G. Quellec, M. Lamard, P.M. Josselin, G. Cazuguel, B. Cochener, C. Roux, Detection of lesions in retina photographs based on the wavelet transform, in: Engineering in Medicine and Biology Society, 2006. EMBS'06. 28th Annual International Conference of the IEEE, vol. 1, 2006, pp. 2618–2621.
[32] M. Niemeijer, B. Ginneken, F. Haar, Automatic detection of the optic disc, fovea and vascular arch in digital color photographs of the retina, in: Proceedings of the British Machine Vision Conference, 2005, pp. 109–118.
[33] K.A. Vermeer, M. Vos F., H.G. Lemij, et al., A model based method for retinal blood vessel detection, Computers in Biology and Medicine 34 (2004) 209–219.
[34] H. Li, W. Hsu, M. Li Lee, Ho. Wang, A piecewise Gaussian model for profiling and differentiating retina vessels, in: Proceedings of ICIP-2003, vol. 1, 2003, pp. 69–72.
[35] L. Gang, O. Chutatape, S.M. Krishnan, Detection and measurement of retinal vessel in fundus images using amplitude modified Gaussian filters, IEEE Transactions on Biomedical Engineering 49 (2002) 168–172.
[36] A. Osareh, M. Mirmehdi, B. Thomas, R. Markham, Comparison of color spaces for optic disc localization in

Please cite this article in press as: C. Köse, et al., Simple methods for segmentation and measurement of diabetic retinopathy lesions in retinal fundus images, Comput. Methods Programs Biomed. (2011), doi:10.1016/j.cmpb.2011.06.007

retinal images, in: Proc. 16th IEEE Int. Conf. Pattern Recognition, vol. 1, 2002, pp. 743–746.
[37] M. Al-Rawi, M. Qutaishat, M. Arrar, An improved matched filter for blood vessel detection of digital retinal images, Computers in Biology and Medicine 37 (2007) 262–267.
[38] R. Chrastek, M. Wolf, K. Donath, et al., Automated segmentation of the optic nerve head for diagnosis of glaucoma, Medical Image Analysis 9 (2005) 297–314.
[39] F. Mendels, C. Heneghan, P.D. Harper, R.B. Reilly, J.-Ph. Thiran, Extraction of the optic disk boundary in digital fundus images, in: Proc.1st Joint BMES/EMBS Conf., 1999, p. 1139.
[40] K. Akita, H.A. Kuga, Computer method of understanding macular fundus images, Pattern Recognition 15 (1982) 1–443.
[41] W.E. Hart, B. Cote, P. Kube, M. Goldbaum, M. Nelson, Automatic segmentation and classification of objects in retinal images, Computer Science and Engineering, University of California, San Diego, June 24, 1994, pp. 171–172.
[42] C. Sinthanayothin, Vi. Kongbunkiat, S. Phoojaruenchanachai, A. Ingalavanija, Automated screening system for diabetic retinopathy, in: Proc. lSPAO3, 2003, pp. 915–920.
[43] J.A. Xu, O. Chutatape, Auto-adjusted 3-D optic disk viewing from low-resolution stereo fundus image, Computers in Biology and Medicine 36 (2006) 921–940.
[44] M.J. Cree, J.A. Olson, K.C. McHardy, et al., A fully automated comparative microaneurysm digital detection system, Eye 11 (1997) 622–628.
[45] J. Nayak, P.S. Bhat, U.R. Acharya, et al., Automated identification of diabetic retinopathy stages using digital fundus images, Journal of Medical Systems 32 (2008) 107–115.
[46] C. Köse, Fully automatic segmentation of coronary vessel structures in poor quality X-ray angiograms images, Lecture Notes in Computer Science, LNCS (Springer) 4109 (2006) 72–82.
[47] C. Köse, O. Gençalioğlu, U. Şevik, An automatic diagnosis method for the knee meniscus tears in MR images, Expert System With Applications 36 (2009) 1208–1216, doi:10.1016/j.eswa.2007.11.036.
[48] M. Niemeijer, M.D. Abramoff, B. van Ginneken, Segmentation of the optic disc, macula and vascular arch in fundus photographs, IEEE Transaction on Biomedical Engineering 26 (2007) 116–127.
[49] M.D. Abramoff, W.L.M. Alward, E.C. Greenlee, et al., Automated segmentation of the optic disc from stereo color photographs using physiologically plausible features, Investigative Ophthalmology & Visual Science 48 (2007) 1665–1673.
[50] M. Sonka, V. Hlavac, R. Boyle, Image Processing, Analysis and Machine Vision, Brooks/Cole Publishing Company, 1999.
[51] T. Kayıkçıoğlu, A. Gangal, M. Turhal, C. Köse, A surface-based method for detection of coronary vessel boundaries in poor quality X-ray angiogram Images, Pattern Recognition Letters 23 (2002) 783–802.

Please cite this article in press as: C. Köse, et al., Simple methods for segmentation and measurement of diabetic retinopathy lesions in retinal fundus images, Comput. Methods Programs Biomed. (2011), doi:10.1016/j.cmpb.2011.06.007